# Corrosion and Properties of Developed Ni-CeO₂ Co-deposited on Mild Steel at varying Current Densities

## M.F Phala[a*], A.P.I. Popoola[a], O.S.I. Fayomi[a, b]

*ᵃDepartment of Chemical, Metallurgical & Materials Engineering, Tshwane University of Technology, P.M.B X680, Pretoria, South Africa*
*ᵇDepartment of Mechanical Engineering, Covenant University, P.M.B. 1023, Canaan land, Ota, Nigeria*

**Abstract**

Rare earth Nickel composite film was attempted on mild steel surface by DC electrodeposition for improvement of corrosion resistance and morphological structure. A conventional Watts bath was utilised for film fabrication and rare earth cerium oxide particle reinforcement were made at 5g/l $CeO_2$ addition to the plating bath. The effect of varying current density (1.0-2.0 A/dm²) on coating morphology was studied by a Scanning Electron Microscope (SEM) and Linear polarization technique for corrosion resistance studied in 3.65% simulated saline environment ($Cl^-$ nature). Coatings exhibited improved corrosion resistance compared to pure Nickel coatings. Increase in current density was observed to result in improved resistance to corrosion. SEM/EDX results revealed presence of Ce metal in coating owing to the inclusion of $CeO_2$ particles in plating bath and evidence of particle agglomeration.

## 1. Introduction

Electrodeposition technique can be utilized for fabrication of matrix composite coatings where insoluble materials are suspended in an electrolytic plating bath and thus captured in the developing matrix during deposition [1]. This method boasts the advantage of low operating cost, low temperature, ease of use as well as being a single-step process where thermal treatment is eliminated [2], [3]. Coatings are fabricated through co-deposition of polymer or fine ceramic particles in a metal matrix using an electrolytic bath [4]. Composite electrodeposition

---

* Phala M.F. Tel.: +27-012-382-4663.
E-mail address: mookanephala@gmail.com

technique has proven to be a low-cost process that operates at low temperatures and producing thus films with excellent coating properties like wear and abrasion resistance [5]. The inclusion of nano-sized particles into developing matrix provides for promotion of coating homogeneity while expanding forward potential applications of composite coatings [6].

Nickel, one of the most widely and commonly used structural metal in the engineering world, can be used for coatings that provide for erosion, abrasion and corrosion resistance. To further improve such existing properties, composite coatings have been thus developed [6] Considerable research contributions have been made and devoted to improvement of properties of electrodeposited Nickel and Nickel alloys, including as well, co-deposition of second-phase inert particles forming as a result, nanocomposite coating, modification of process parameters and employing pulse electrodeposition route [7]. Incorporation of second-phase solid particles in nickel electrodeposition bath disturbs continual growth of nickel crystals through introduction of new nucleation sites leading to formation of fine crystalline coating which results in improvement of anticorrosion properties of coatings [8]. For composite co-deposition, $CeO_2$ has attracted considerable attention in metal-matrix composite films [9]. Rare earth compounds find a wide use in a variety of applications owing to their special chemical and physical characteristics. Ceria is one of the powerful rare earth oxides as it boasts combination superior properties like corrosion resistance and wear properties [1]. According to [10] inclusion of $CeO_2$ particles in nickel metal matrix led to an improved wear resistance, high temperature oxidation as well as an improved corrosion resistance compared to pure nickel coating. The purpose of the study at hand is property improvement of pure nickel coatings by Ceria particle reinforcement employing low current densities.

| Nomenclature | |
|---|---|
| A | Control Sample |
| B | Test Sample |

## 2. Experimental

Mild steel sectioned sheets of dimension (5x5x2 mm) were grinded as part of pre-plating surface preparation step. SiC emery paper of grit 60μm, 120μ, 360μ, 400μm and 1600μm were used respectively to aid in achieving uniform and dent-free working surface. Following subsequent polishing, 2 M HCl was used to activate the coating surface through dipping after which the surface was further rinsed with deionized water.

Electrodeposition process was conducted with Agilent U8002A 0-30V, 5A Laboratory single output DC rectifier. Using deionized water, a Watts bath was prepared in a 1l laboratory glass beaker utilizing analytical grade chemical constituents of a proper Watts plating solution. Watts plating solution consisted of 300g/l $NiSO_4.6H_2O$, 40g/l $NiCl_2.6H_2O$ and 35g/l $H_3BO_3$. The polished mild steel sectioned sheets of dent-free mirror finish served as cathode and 99.9% Nickel anodes placed 5 cm apart served as conduction anodes for electron transportation and transfer. $CeO_2$ additions were made at 5 g/l to plating solution and deposition time was maintained at 10 minutes. The plating current was thus varied in the order 1.0 A/dm$^2$, 1.5 A/dm$^2$ and 2.0 A/dm$^2$ respectively while a DRAGONLAB (MS-H-Pro) Stirrer/Heater was used to aid in particles suspension by stirring and a constant 400 rpm stirring rate. Plated samples were washed with running tap water and air dried for 24 hours before storage.

The coating surface morphology analysed with a high resolution Scanning Electron Microscope (SEM-JSM 7600F) equipped with field emission cathode Energy Dispersive X-ray (EDX).

Table 1: Watts Bath Chemical Constituents

| Material | Composition (g/l) | Plating Parameter | Unit, Value |
|---|---|---|---|
| $NiSO_4.6H_2O$ | 300 | Temperature | 25˚C±3 |
| $NiCl_2.6H_2O$ | 40 | pH | 4.0-5.5 |
| $H_3BO_3$ | 35 | Stirring Rate | 400 rpm |
| $CeO_2$ | 5 | Current Density | 1.0-2.0 A/dm$^2$ |
| | | Deposition Time | 10 mins |

An AutoLab Type (III) Potentiostat/Galvanostat with a 3M KCl electrode and graphite reference electrode was used to test the corrosion resistance of the coatings in a 3.65% simulated corrosive saline environment were the obtained corrosion performance data was interpreted with the aid of Nova Version 1.8 computerised software.

## 3. Results and Discussion
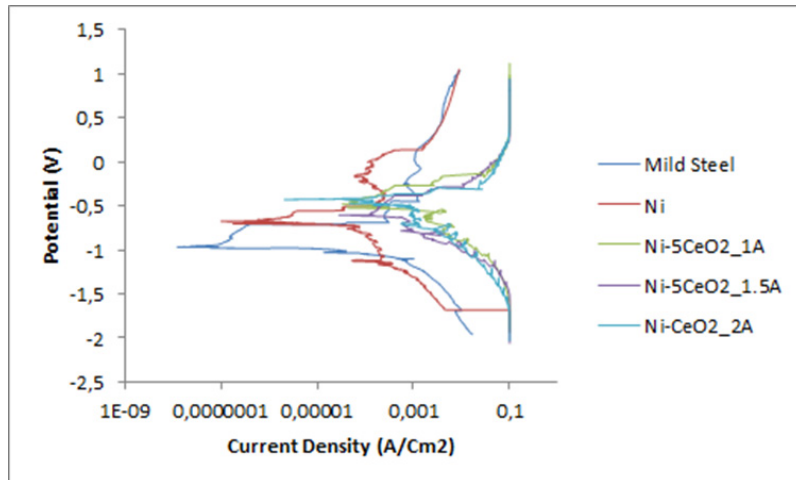
### 3.1. Corrosion Resistance and Linear polarization



Figure 1: Tafel curves of Mild Steel, Pure Nickel and Ni-5CeO$_2$ coatings

Table 2: Tafel curve corrosion data

|  | Ecorr, Calc (V) | Ecorr, Obs (V) | icorr (A) | Corrosion rate (mm/year) | Polarization resistance (Ω) |
|---|---|---|---|---|---|
| Mild Steel | -1,0486 | -0,97864 | 0,00085011 | 9,8782 | 232,56 |
| Pure Nickel | -0,66927 | -0,70976 | 0,00019881 | 2,3102 | 1620,5 |
| Ni-5CeO$_2$_1A | -0,66741 | -0,48333 | 7,26E-05 | 0,84374 | 615,35 |
| Ni-5CeO$_2$_1,5A | 0,9491 | -0,44881 | 0,00010591 | 1,2307 | 916,26 |
| Ni-5CeO$_2$_2A | -0,63217 | -0,69623 | 2,86E-05 | 0,33279 | 891,96 |

As depicted in Table 3, the values of Ecorr for mild steel and pure nickel coatings were -978.64mV, -709.76mV while Icorr values were registered at 0.085011mA and 0.019881mA respectively. As also observed by [11], addition of CeO$_2$ (g/l) particles resulted in thus a decrease in Ecorr and Icorr values. According to [3] this proves that Ni-xCeO$_2$ (x=5 g/l) is more noble than mild steel and Ni. This effect resulted in an increase in coating efficiency as observed in figure 2 exhibiting the effectiveness of the coating. The introduction of CeO$_2$ into the plating bath increased the surface area of inert particles on the coating surface. Consequently, Tafel plot values concurred with Tafel curves proving that Ni-5CeO$_2$ coated at 2A/dm$^2$ to be having the highest resistance to corrosion, depicted also by an averaging low corrosion rate.
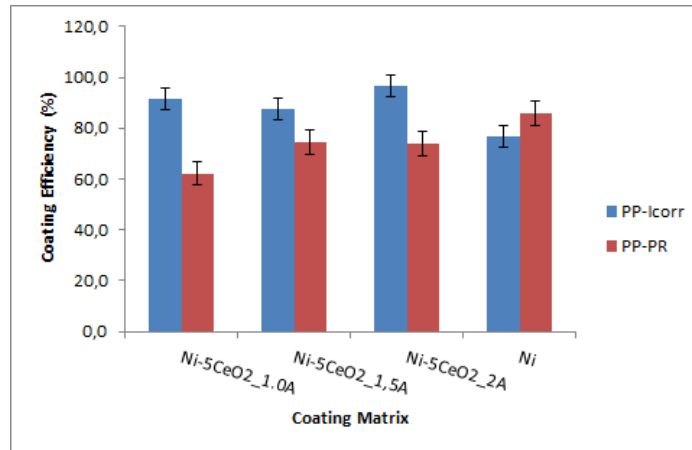
## 3.2. Coating efficiency



Figure 2: Coating Efficiency of Pure Nickel and Ni-5CeO$_2$ Coatings

Coating efficiencies of the electrodeposited coatings were calculated using the following formulae:

$$CE_{Icorr} = \frac{Icoor(A) - Icoor(B)}{Icoor(A)} \times 100\% \tag{1}$$

$$CE_{PR} = \frac{PR(B) - PR(A)}{PR(B)} \times 100\% \tag{2}$$

Improved corrosion resistance at 2A/dm$^2$ compared to 1.0A.dm$^2$ and 1.5A/dm$^2$ was consequence to further growth in film thickness imbedding thus, appreciable amount of inert CeO$_2$ particles in the growing matrix. The result was further attributed to the high corrosion resistance of CeO$_2$ [12] and its protection action [13]. This increases thus the chances of localised micro-corrosion cells on the film coating. To mention but a few, [11], [13], and [14] reported an increase in corrosion resistance with inclusion of Ceria particle reinforcement in Nickel matrix. CeO$_2$ particles were deposited on the cathode surface through adsorption [15].

## 3.3. Optical Microscopy

Figure 3(a) below depicts Optical Microscopic imaging of pure nickel coating produced from a Watts bath. Coating surface contains no visible surface defects such as cracks and macro-pores, while Figure 3 (b) of Ni-5CeO$_2$ produced at 2A/dm$^2$ for 10 minutes shows evidence of agglomerated CeO$_2$ particles [7]. Reinforcement of surface resulted in elimination of possible defects and compaction of the microstructure.
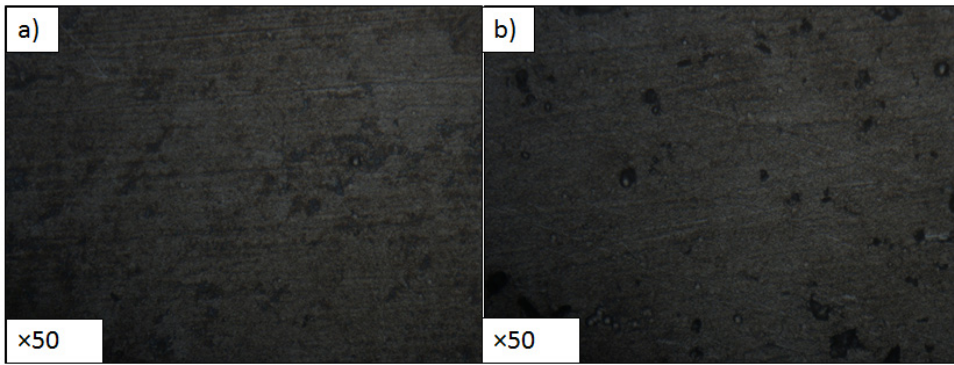
Figure 3: a) OM imaging of Pure Nickel Surface Coating; b) OM imaging of Ni-5CeO$_2$ Coating Deposited at 2A/dm$^2$
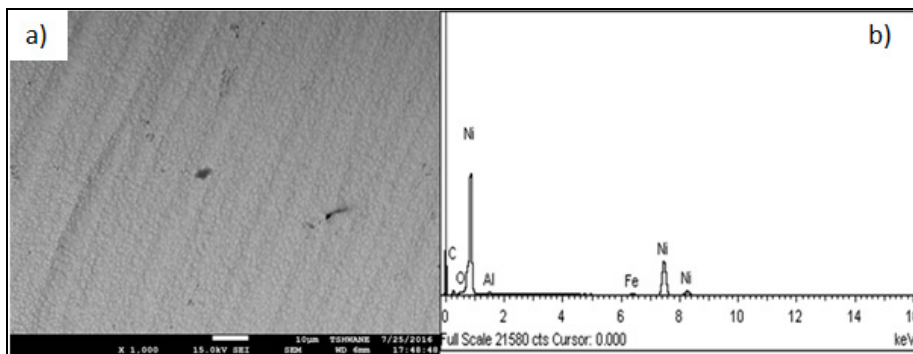
### 3.4. SEM/EDS analysis



Figure 4: SEM/EDS imaging of pure nickel coating on Mild steel surface

Figure 4 represents SEM/EDX imaging of pure nickel coating deposited on mild steel surface. Figure 4(b) depicts presence on Ni deposited on surface coating and as well, traces of Iron attributed to presence of micropores. The surface reveals a well compact surface coating with minimal process defects and a characteristic cauliflower-like morphology and refined structure.

Pure Nickel coatings are also characterized by growth of larger grain sizes compared to reinforced layers which have new nucleation sites developing due to disturbance points caused by reinforcing particles (CeO$_2$) which are only embedded in the growing nucleation field. Embedding of particles leads as well to grain refinement of the growing metallic matrix. Ni crystalline size decreases with inclusion of CeO$_2$ particles in Ni matrix and hence coating thickness.

During electrodeposition, Ceria particles absorb cations from the bath under high potential gradient [10]. However; agglomeration on the surface leads to formation of protruding structures or clusters [5] a phenomenon which can lead to deterioration of mechanical properties, in particular, wear resistance due to an increase in surface roughness. Figure 5 of 2A/dm$^2$ Ni-CeO$_2$ (5 g/l) reveals presence of as such, agglomerated Ceria particle species.
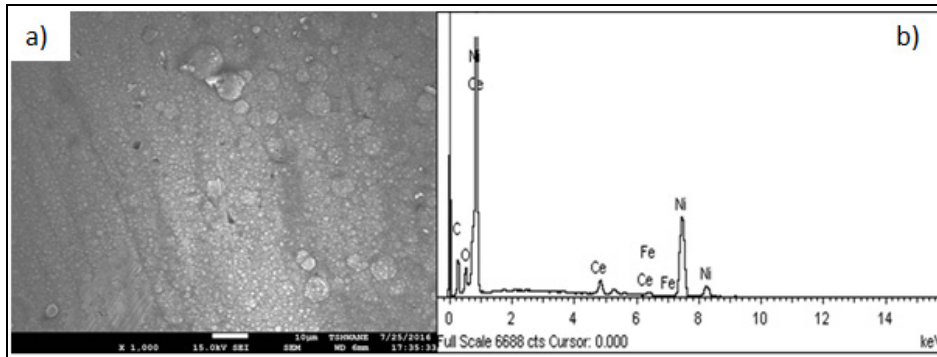
Figure 5: SEM/EDS imaging of Ni-CeO$_2$ (5 g/l) at 2 A/dm$^2$

## 4. Conclusion

Nickel-ceria composite was successfully developed on mild steel surface utilizing a Watts bath at ambient temperatures. The resulting coating exhibited:

- An increase in corrosion resistance at varying current density in the order 1.5, 1.0 and 2.0 A/dm2 proving the coating can be utilized for the purpose of surface protection and corrosion mitigation.
- The fabricated coatings had a minimal presence of surface defects and a well refined grain structure revealed through Scanning Electron Microscope analysis.

## Acknowledgements

## References

[1] Y.J. Xue, X.Z. Jia, Y.W. Zhou, W. Ma, J.S. Li, Surf. Coat. Tech. 200 (2006) 5677-5681.
[2] M. Schlesinger, M. Paunovic, Modern Electroplating, John Wiley & Sons, Inc., Hoboken, New Jersey, USA, 2010.
[3] S.T. Aruna, P.V.K. Srikanth, M. Jamil Ahamad, S. Latha, K.S. Rajam, Portu. Electrochim. Acta 29(1) (2011) 23-27.
[4] S.T. Aruna, C.N. Bindu, V. Ezhil Selvi, V.K. William Grips, K.S. Rajam, Surf. Coat. Tech. 200 (2006) 6871-6880.
[5] B. Tushar, P.H. Sandip, J. Coat. Tech. 205 (2011) 4124-4134.
[6] N.S. Qu, W.H. Qian, X.Y. Hu, Z.W. Zhu, Int. J. Electro. Sci. 8 (2013) 11545-11577.
[7] C. Xiong, Y. Wang, B. Hu, L. Chen, S.L. Tay, A. Xu, W. Gao, Int. J. Electro. Sci. 11(2016) 906-914.
[8] B. Szczygiel, M. Kolodziej, Electrochim .Acta 50 (2005) 4188-4195.
[9] Y.B. Zheng, N.S. Qu, X.Y. Hu, Int. J. Electro. Sci. 9 (2013) 8145-8154.
[10] N.S. Qu, D. Zhu, K.C. Chan, Scripta Mater. 54 (2006) 1421-1425.
[11] Y.B. Zeng, N.S. Qu, X.Y. Hu, Int. J. Electrochem. Sci. 9 (2014) 8145-8154.
[12] M. Srivastava, V.K. William Grips, K.S. Rajam, Appl. Surf. Sci. 257 (2010) 717-722.
[13] N. Cioatera, A. Samide, A. Maxut, R.N. Vannier, M. Traisnel, Rev. Roum. Chim. 56(10-11) 1003-1009.
[14] S. Kasturibai, G. Paruthimal Kalaignan, Mater. Chem. Physic. 147 (2014) 1042-1048.
[15] Y.J. Xue, H.B. Liu, M.M. Lan, J.S. Li, H. Li, Surf. Coat. Tech. 204 (2010) 3539–3545.